

Syntheses, structure, reactivity and species recognition studies of oxo-vanadium(v) and -molybdenum(vi) complexes †

Chebrolu P. Rao,^{*,a} Alavattam Sreedhara,^a P. Venkateswara Rao,^a M. Bindu Verghese,^a Kari Rissanen,^b Erkki Kolehmainen,^b N. K. Lokanath,^c M. A. Sridhar^c and J. Sashidhara Prasad^c

^a *Bioinorganic Laboratory, Department of Chemistry, Indian Institute of Technology Bombay, Powai, Mumbai - 400 076, India*

^b *Department of Chemistry, University of Jyväskylä, Fin 40351, Jyväskylä, Finland*

^c *Department of Studies in Physics, University of Mysore, Manasagangothri, Mysore - 570 006, India*

Alkoxo-rich Schiff-bases of potentially tri-, tetra- and penta-dentate binding capacity, and their sodium tetrahydroborate-reduced derivatives, have been synthesized. Their oxo-vanadium(v) and -molybdenum(vi) complexes were synthesized and characterized using several analytical and spectral techniques including multinuclear NMR spectroscopy and single-crystal X-ray diffraction studies. Eight structurally different types of complexes possessing distorted square-pyramidal, trigonal-bipyramidal and octahedral geometries have been obtained. While V^{VO} exhibits dimeric structures with 2-HOC₆H₄CH=NC(CH₂OH)₃ and 2-HOC₆H₄CH₂-NHC(CH₂OH)₃ and related ligands through the formation of a symmetric V₂O₂ core as a result of bridging of one of the CH₂O⁻ groups, Mo^{VI}O gives only mononuclear complexes even when some unbound CH₂OH groups are available and the metal center is co-ordinatively unsaturated. In all the complexes the nitrogen atom from a HC=N or H₂CNH group of the ligand occupies a near *trans* position to the M=O bond. While the Schiff-base ligands act in a tri- and tetra-dentate manner in the vanadium(v) complexes, they are only tridentate in the molybdenum(vi) complexes. Proton NMR spectra in the region of bound CH₂ provides a signature that helps to differentiate dinuclear from mononuclear complexes. Carbon-13 NMR co-ordination induced shifts of the bound CH₂ group fit well with the charge on the oxometal species and the terminal or bridging nature of the ligand. The reactivity of the vanadium(v) complexes towards bromination of the dye xylene cyanole was studied. Transmetallation reactions of several preformed metal complexes of 2-HOC₆H₄CH=NC(CH₂OH)₃ with VO³⁺ were demonstrated as was selective extraction of VO³⁺ from a mixture of [VO(acac)₂] and [MoO₂(acac)₂] using this Schiff base. The unusual selectivity and that of related derivatives for VO³⁺ is supported by binding constants and the solubility of the final products, and was established through a.c. conductivity measurements. The *cis*-MoO₂²⁺ complexes with alkoxo binding showed an average Mo–O_{alk} distance of 1.926 Å, a value that is close to that observed in the molybdenum(vi) enzyme dmsoreductase (1.92 Å). Several correlations have been drawn based on the data.

Oxometal cationic species, such as VO²³⁺, VO₂⁺ and MoO₂²⁺, have pronounced three-dimensional anisotropy which in principle is expected to be reflected in their co-ordination chemistry, particularly through selective complexation followed by species recognition. Selectivity of metal complexation is a chemical feature of certain ligands that may find importance in a number of fields, such as bioinorganic chemistry,¹ environmental science and even in metal ore processing.

The involvement and importance of vanadium and molybdenum particularly as oxometal species in their respective metalloenzymes in biological systems is well recognized² and has led to renewed interest in the chemistry of oxo-vanadium(v) and -molybdenum(vi) model compounds.³ Furthermore the VO₂⁺ species are implicated in the brominating activity of model compounds in acidic media in the presence of peroxide.⁴ On the other hand, sea squirts (ascidians) are known to accumulate large concentrations of vanadium from sea-water selectively where the concentration of molybdenum is in at least fivefold excess over that of vanadium, although vanadium exhibits no specific function. Both the vanadium and molybdenum are present in their highest oxidation states, possibly as oxo species in sea-water. Once the vanadium is accumulated by

these species it is stored in the vanadocytes of sea squirts bound to tunicochromes possessing phenoxo and amide moieties.⁵ However, the selective extraction of vanadium from sea-water by these species is still not understood.

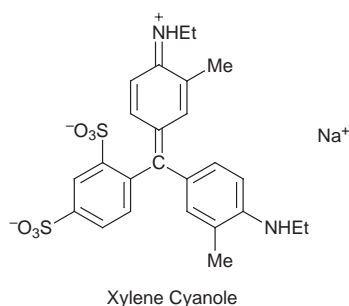
The EXAFS and/or crystal structures of vanadium-containing bromoperoxidase⁶ and molybdenum-containing dmsoreductase^{7,8} (both in the reduced and oxidized forms of the enzyme) have indicated the involvement of alkoxo moieties, perhaps arising from serine in the metal co-ordination sphere, in addition to the oxometal moieties, based on the bond distances. However, there are no reports of crystal structures of small model molecules supporting these bond parameters, though the existence of such data would have immense value.

All these aspects unambiguously infer the presence and involvement of oxo-vanadium and oxo-molybdenum centers in a number of biological processes. Therefore the studies reported in this paper are mainly designed to address the role of oxometal centers which are particularly influenced by the binding of alkoxo moieties. Such efforts are certainly expected to throw light on the issues discussed in this introduction. Thus, in the present paper we have focused our attention on the synthesis of a number of new types of oxo-vanadium(v) and molybdenum(vi) complexes and their reactivity towards bromination. Further, the studies also address the selective recognition of oxo-vanadium(v) over molybdenum(vi). In order to achieve meaningful results, the ligands have been designed accordingly to possess one, two or even three CH₂OH moieties.

† Supplementary data available: graphical correlations, absorption spectra and stereoviews. Available from BLDSC (No. SUP 57388, 8 pp.). See Instructions for Authors, 1998, Issue 1 (<http://www.rsc.org/dalton>).

Experimental

The labeling, structures of the ligands used, and the chemical composition of the complexes synthesized and those crystallographically characterized are listed in Scheme 1. Salicylaldehyde (Hsal), 2-amino-2-methylpropan-1-ol (amp), 2-amino-2-methylpropan-1,3-diol (ampd), tris(hydroxymethyl)aminomethane (Tris), triethanolamine (H₃tea), NH₄VO₃, phenol red and acetylacetonone (Hacac) were from Loba Chemie (India) and distilled or recrystallized before use. Xylene cyanole, *N*-[tris(hydroxymethyl)methyl]glycine (tricine) (Sigma Chem. Co.), VOSO₄, H₂O₂ and KBr (E. Merck) were used as received. The Schiff bases (Scheme 1) were synthesized as reported earlier by us.^{9–11} The complexes [Mn^{IV}-(H₂L⁷)₂],¹² [Mn^{II}Mn^{III}L⁷(O₂CMe)₄(MeOH)₂],¹³ [VO(salamq)-(cat)]^{11b} (where salamq is a Schiff base derived from the 1 + 1 condensation of 8-aminoquinoline and Hsal and cat is catechol), [VO(HL⁸)₂],⁹ [VO₂(H₂L¹⁰)],¹⁴ and [VO(hnanth)-(OMe)(MeOH)]^{11c} (where hnanth is a Schiff base derived from the 1 + 1 condensation of 2-hydroxy-1-naphthaldehyde and anthranilic acid), [VO(tea)] **27**,¹⁵ [VO(acac)₂],¹⁶ [VO(OEt)₃]¹⁰ and [MoO₂(acac)₂]¹⁷ were synthesized as reported elsewhere.

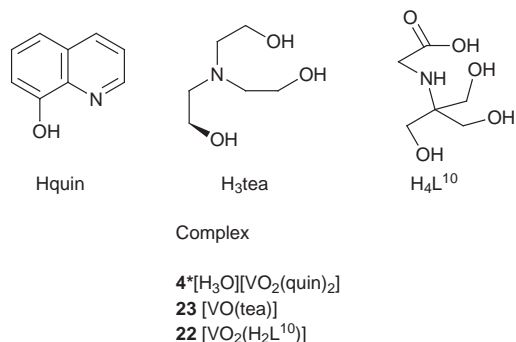
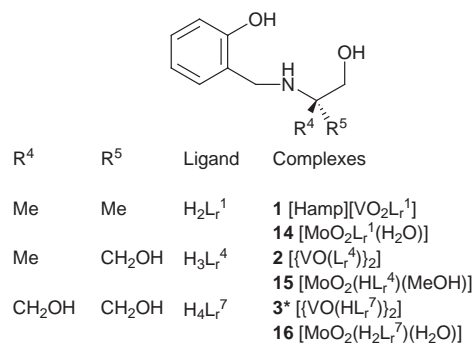
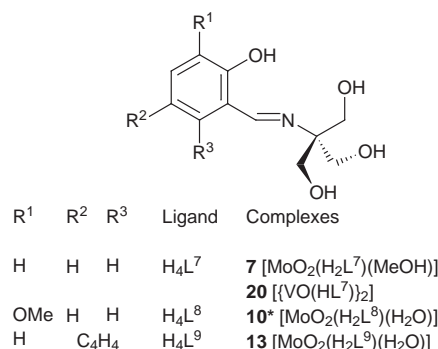
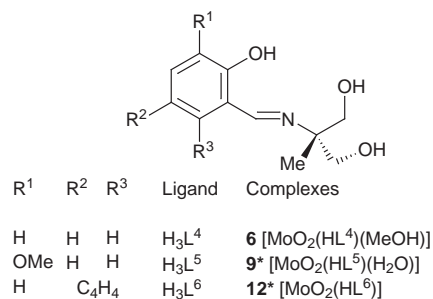
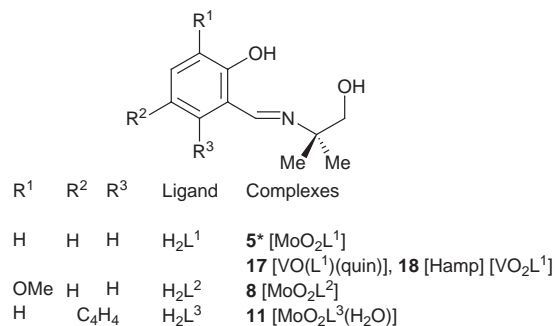


Physical and spectroscopic studies

Fourier-IR, electronic spectra and cyclic voltammetry were obtained as detailed elsewhere,^{9–11} unless otherwise mentioned. The ¹H, ¹³C and ⁵¹V NMR spectra were recorded in (CD₃)₂SO using a Bruker DPX250 spectrometer,⁹ ⁹⁵Mo NMR spectra in (CD₃)₂SO with a Bruker DRX500 (32.59 MHz) and an anti-ringing pulse program to eliminate baseline rolling (the number of scans was varied from 100 000 to 400 000 and an exponential window function of 50 Hz was used prior to FT to improve the signal-to-noise ratio). The ⁹⁵Mo NMR chemical shifts were referenced to the signal of 0.2 M Na₂MoO₄ in water, δ(Na₂MoO₄) 0.

Synthesis of reduced Schiff bases

H₄L_r⁷. To Hsal (10 mmol, 1.221 g) in MeOH (25 cm³) was added solid Tris (10 mmol, 1.21 g). The deep yellow solution which resulted was refluxed for 60 min then cooled to 0 °C and NaBH₄ (10 mmol, 0.39 g) added over a period of 30 min. Slowly the temperature was raised to room temperature. A pale yellow solution resulted and was stirred for 60 min. The solvent was removed *in vacuo* and sodium acetate (2 g) in water (25 cm³) was added and extracted with CHCl₃ or CH₂Cl₂ to give H₄L_r⁷ in about 90% yield. In another procedure, the sample was acidified with hydrochloric acid and extracted with CHCl₃ or CH₂Cl₂ to give H₄L_r⁷·2HCl. The compounds H₂L_r¹ and H₃L_r⁴ were synthesised by adopting the same procedure. ¹H NMR: H₂L_r¹, δ 1.02 (s, 6 H, CH₃), 3.81 (s, 2 H, CH₂OH), 3.26 (s, 2 H, CH₂NH), 4.86 (br, 2 H, NH/OH) and 6.63–7.07 (m, 4 H, aromatic); H₃L_r⁴, 0.72 (s, 3 H, CH₃), 3.36–3.51 (m, 4 H, CH₂OH + CH₂NH), 3.80 (s, 2 H, CH₂OH), 5.70 (br, NH/OH) and 6.60–7.05 (m, 4 H, aromatic); H₄L_r⁷, 3.25–3.32 (d, 1 H), 3.45–3.67 (m, 4 H, CH₂OH + CH₂NH), 4.03 (br, 3 H, CH₂OH), 4.45–4.55 (t, 1 H) and 6.68–7.12 (m, 4 H, aromatic).



Scheme 1 Ligands used and complexes synthesized, * indicates a single-crystal structure determination, subscript r the presence of amine (CH₂NH) in place of imine (CH=N)

Synthesis of vanadium complexes

[Hamp][VO₂L_r¹] 1. The complex [VO(acac)₂] (2 mmol, 0.53 g) was added to a mixture of H₂L_r¹ (2 mmol, 0.390 g) and amp (2 mmol, 0.18 g) in MeOH (15 cm³) and refluxed for 6 h, resulting in a pale yellow solution. When the solvent was completely

removed *in vacuo* a yellow paste resulted which was triturated using MeCN. The clear solution was stored at 0 °C for 7 d to give pale yellow microcrystalline material in 55% yield (Found: C, 49.45; H, 7.01; N, 7.50; V, 14.45. Calc. for C₁₅H₂₇N₂O₅V: C, 49.19; H, 7.38; N, 7.65; V, 13.92%). ¹H NMR: δ 1.024, 1.17, 1.14 (12 H, CH₃), 3.27 (free CH₂OH), 3.74 (bound CH₂O⁻), 3.81 (2 H, CH₂NH), 4.98 (NH) and 6.47–7.06 (aromatic). ⁵¹V NMR: δ -509.8 and -518.9. FTIR (in KBr matrix, cm⁻¹): ν(OH) 3404, ν(NH) 3207; ν(V=O) 935, 854. UV/VIS (dmf): λ/nm (ε/M⁻¹ cm⁻¹) 261 (5381), 278 (6919) and 324 (2621).

[VO(L_r⁴)₂]2**. To H₃L_r⁴ (2 mmol, 0.422 g) in MeOH (10 cm³) was added [VO(acac)₂] (2 mmol, 0.530 g) and refluxed for 4 h. The deep red solution obtained was removed *in vacuo* and an excess of diethyl ether added to precipitate a red-brown solid. This was washed with MeOH, thrice for 6 h each time and finally dried *in vacuo*. The same complex was also synthesized using Na₃VO₄ or [VO(OEt)₃]. All attempts to isolate and characterize it as a pure solid were unsuccessful due to its hydrolytic instability. FTIR (KBr matrix, cm⁻¹): ν(NH) 3263, ν(V=O) 958 ⁵¹V NMR: δ -388.4 (65%), -444, -498 and -512.6 (35%).**

[VO(HL_r⁷)₂]3**. To H₄L_r⁷ (5 mmol, 1.135 g) in MeOH (25 cm³) was added [VO(acac)₂] (5 mmol, 1.325 g) and refluxed for 4 h. A red-brown precipitate was filtered off and purified as for **1** to obtain the product **3** in 67% yield. The same complex can be prepared from Na₃VO₄ or [VO(OEt)₃] (Found: C, 44.97; H, 4.86; N, 4.57; V, 17.62. Calc. for C₁₁H₁₄NO₅V: C, 45.37; H, 4.81; N, 4.81; V, 17.51%). ¹H NMR: δ 3.41–3.75 (m, 4 H, CH₂-OH + CH₂NH), 3.96 (d, 1 H, CH₂O⁻), 4.29 (d, 1 H, CH₂O⁻), 4.86 (d, 1 H, CH₂O⁻), 5.15 (t, 1 H, free OH), 5.27 (d, 1 H, CH₂O⁻), 5.46 (br, NH) and 6.83–7.32 (m, 4 H, aromatic). ⁵¹V NMR: δ -395.5 (90) and -504 (10%). FTIR (KBr matrix, cm⁻¹): ν(OH) 3403, ν(NH) 3277, ν(V=O) 961. UV/VIS (dmf): λ/nm (ε/M⁻¹ cm⁻¹) 474 (7401), 300 (8379) and 262 (12 401). Single crystals suitable for X-ray diffraction studies was obtained as [VO(HL_r⁷)₂]**2**dmf from a concentrated solution in dmf at ~4 °C after 5 d.**

[H₃O][VO₂(quin)₂]4**. From a reaction mixture containing [VO(acac)₂], H₃L¹ and Hquin in MeOH, [VO(L¹)(quin)] was isolated as described elsewhere.⁹ From the filtrate of this reaction mixture, yellow crystals of **4** were isolated in about 20–25% yield. Recrystallization from MeOH yielded single crystals suitable for X-ray studies (Found: C, 53.02; H, 4.32; N, 6.61; V, 12.86. Calc. for C₁₈H₁₇N₂O₆V: C, 52.95; H, 4.17; N, 6.86; V, 12.49%). ¹H NMR: δ 6.83–8.30. ¹³C NMR: δ 110.6–165.2. ⁵¹V NMR: δ -520.5. FTIR (KBr matrix, cm⁻¹): ν(OH) 3400, 3287; ν(V=O) 910, 880. UV/VIS (dmf): λ/nm (ε/M⁻¹ cm⁻¹) 264 (29 545), 337 (4427) and 378 (5460).**

Complex **4** was also isolated from a reaction mixture containing [VO(acac)₂], H₃L⁴ or H₄L⁷ and Hquin in MeOH in 8–10% yields. The major products in the above reactions are the VO³⁺ dimers of the respective Schiff bases, [VO(L⁴)₂] or [VO(HL⁷)₂] which were isolated in about 70–80% yields. However, no mixed-ligand complex of VO³⁺ with H₃L⁴ or H₄L⁷ as the Schiff base and Hquin as coligand was isolated.

Synthesis of molybdenum complexes

[MoO₂L¹]5**. To H₂L¹ (0.384 g, 2 mmol) in MeOH (10 cm³) was added [MoO₂(acac)₂] (0.656 g, 2 mmol) and the reaction mixture stirred at room temperature for 6 h. A yellow precipitate formed which was filtered off and washed by stirring in MeOH for 6 h. This was repeated thrice before drying the sample *in vacuo* (Found: C, 41.44; H, 4.22; Mo, 30.38; N, 4.36. Calc. for C₁₁H₁₃MoNO₄: C, 41.38; H, 4.08; Mo, 30.08; N, 4.39%). ¹H NMR: δ 8.65 (imine), 7.66–6.87 (m, aromatic), 4.26 (s, 2 H, CH₂OH) and 1.37 (s, 6 H, CH₃). ¹³C NMR: δ 162.01 (imine), 159.73–119.05 (aromatic), 84.06 (bound CH₂O⁻), 67.33 (ter-**

tiary C) and 25.23 (CH₃). ⁹⁵Mo NMR: δ 30.9, FTIR (KBr matrix, in cm⁻¹): ν(OH) 3400; ν(C=N) 1629; ν(MoO₂) 931, 912. UV/VIS (dmf): λ/nm (ε/M⁻¹ cm⁻¹) 263 (17 303) and 346 (1503). Complexes **6–16** were synthesized and purified as for **5**.

[MoO₂(HL⁴)(MeOH)]6** (Found: C, 36.91; H, 4.19; Mo, 27.39; N, 3.87. Calc. for C₁₁H₁₅MoNO₆: C, 37.40; H, 4.25; Mo, 27.18; N, 3.97%). ¹H NMR: δ 8.53 (s, 1 H, imine), 7.67–6.88 (m, aromatic), 5.07 (t, 1 H, free CH₂OH), 4.57, 4.04 (d, 2 H, CH₂O⁻), 3.53–3.40 (m, 2 H, free CH₂OH) and 1.33 (s, 3 H, CH₃). ¹³C NMR: δ 162.77 (imine), 159.81–119.12 (aromatic), 79.96 (bound CH₂O⁻), 70.76 (tertiary C), 65.16 (free CH₂OH) and 18.63 (CH₃); ⁹⁵Mo NMR: δ 29.6; FTIR (KBr matrix, in cm⁻¹) ν(OH) 3326, 3172; ν(C=N) 1629; ν(MoO₂) 929, 889; UV/VIS (dmf): λ/nm (ε/M⁻¹ cm⁻¹) 273 (17 549) and 346 (4194).**

[MoO₂(H₂L⁷)(MeOH)]0.5H₂O** **7** (Found: C, 36.45; H, 3.89; Mo, 26.65; N, 3.90. Calc. for C₁₁H₁₄MoNO_{6.5}: C, 36.67; H, 4.19; Mo, 27.39; N, 3.89%). ¹H NMR: δ 8.49 (s, 1 H, imine), 7.61–6.88 (m, aromatic), 4.97 (t, 2 H, free CH₂OH), 4.45 (s, 2 H, CH₂O⁻) and 3.73–3.62 (m, 4 H, free CH₂OH); ¹³C NMR: δ 163.65 (imine), 159.81–119.05 (aromatic), 76.84 (bound CH₂O⁻), 73.74 (tertiary C) and 61.07 (free CH₂OH); ⁹⁵Mo NMR: δ 31.6; FTIR (KBr matrix, in cm⁻¹) ν(OH) 3414, 3367; ν(C=N) 1625; ν(MoO₂) 929, 889; UV/VIS (dmf): λ/nm (ε/M⁻¹ cm⁻¹) 266 (12 704) and 347 (2419).**

[MoO₂(L²)]0.5H₂O** **8** (Found: C, 40.23; H, 4.25; Mo, 26.91; N, 3.81. Calc. for C₁₂H₁₆MoNO_{5.5}: C, 40.63; H, 4.47; Mo, 26.80; N, 3.91%). ¹H NMR: δ 8.63 (s, 1 H, imine), 7.24–6.86 (m, aromatic), 4.24 (s, 2 H, CH₂O⁻), 3.79 (s, 3 H, OCH₃) and 1.36 (s, 6 H, CH₃); ¹³C NMR: δ 162.01 (imine), 150.01–116.53 (aromatic), 83.99 (bound CH₂O⁻), 67.22 (tertiary C), 55.80 (OCH₃) and 25.21 (CH₃); ⁹⁵Mo NMR: δ 32.1; FTIR (KBr matrix, in cm⁻¹) ν(OH) 3439; ν(C=N) 1633; ν(MoO₂) 935, 847; UV/VIS (dmf): λ/nm (ε/M⁻¹ cm⁻¹) 284 (10 736) and 368 (2788).**

[MoO₂(HL⁵)(H₂O)]0.5H₂O** **9** (Found: C, 36.87; H, 4.43; Mo, 24.26; N, 3.51. Calc. for C₁₂H₁₈MoNO_{7.5}: C, 36.74; H, 4.34; Mo, 24.48; N, 3.57%). ¹H NMR: δ 8.51 (s, 1 H, imine), 7.26–6.86 (m, aromatic), 5.04 (t, 1 H, free CH₂OH), 4.57, 4.02 (d, 2 H, CH₂O⁻) (s, 3 H, OCH₃), 3.57–3.40 (m, 2 H, free CH₂OH) and 1.33 (s, 3 H, CH₃); ¹³C NMR: δ 162.75 (imine), 150.09–116.46 (aromatic), 79.88 (bound CH₂O⁻), 70.64 (tertiary C), 65.17 (free CH₂OH), 55.80 (OCH₃) and 18.59 (CH₃); ⁹⁵Mo NMR: δ 33.2; FTIR (KBr matrix, in cm⁻¹) ν(OH) 3343; ν(C=N) 1621; ν(MoO₂) 924, 893; UV/VIS (dmf): λ/nm (ε/M⁻¹ cm⁻¹) 258 (10 714), 283 (12 382) and 365 (2778).**

[MoO₂(H₂L⁸)(H₂O)]0.5H₂O** **10** (Found: C, 34.65; H, 4.58; Mo, 23.71; N, 3.27. Calc. for C₁₂H₁₉MoNO_{8.5}: C, 34.87; H, 4.60; Mo, 23.32; N, 3.39%). ¹H NMR: δ 8.48 (s, 1 H, imine), 7.17–6.88 (m, aromatic), 4.96 (t, 2 H, free CH₂OH), 4.43 (s, 2 H, CH₂O⁻), 3.79 (s, 3 H, OCH₃) and 3.72–3.61 (m, 4 H, free CH₂OH); ¹³C NMR: δ 163.62 (imine), 150.09–116.39 (aromatic), 76.75 (bound CH₂O⁻), 73.63 (tertiary C), 61.06 (free CH₂OH) and 55.80 (OCH₃); ⁹⁵Mo: δ 34.0; FTIR (KBr matrix, in cm⁻¹) ν(OH) 3473, 3348; ν(C=N) 1624; ν(MoO₂) 934, 903; UV/VIS (dmf): λ/nm (ε/M⁻¹ cm⁻¹) 261 (9729), 283 (12 292) and 364 (2591).**

[MoO₂L³(H₂O)]11** (Found: C, 47.10; H, 4.80; Mo, 24.71; N, 3.40. Calc. for C₁₅H₁₇MoNO₅: C, 46.52; H, 4.39; Mo, 24.79; N, 3.62%). ¹H NMR: δ 9.45 (s, 1 H, imine), 8.53–7.13 (m, aromatic), 4.32 (s, 2 H, CH₂O⁻) and 1.49 (s, 6 H, CH₃); ¹³C NMR: δ 157.05 (imine), 160.51–111.85 (aromatic), 84.27 (bound CH₂O⁻), 68.29 (tertiary C) and 25.43 (CH₃); ⁹⁵Mo NMR: δ 32.5; FTIR (KBr matrix, in cm⁻¹) ν(C=N) 1621; ν(MoO₂) 932, 894; UV/VIS (dmf): λ/nm (ε/M⁻¹ cm⁻¹) 263 (12 437), 305 (12 040) and 381 (3879).**

[MoO₂(HL⁴)]12** (Found: C, 46.33; H, 3.92; Mo, 24.46; N, 3.50. Calc. for C₁₅H₁₅MoNO₅: C, 46.76; H, 3.90; Mo, 24.64; N, 3.64%). ¹H NMR: δ 9.37 (s, 1 H, imine), 8.40–7.15 (m, aromatic), 5.17 (t, 1 H, free CH₂OH), 4.62, 4.16 (d, 2 H, CH₂O⁻), 3.62–3.57 (m, 2 H, free CH₂OH) and 1.47 (s, 3 H, CH₃); ¹³C NMR: δ 157.68 (imine), 160.60–111.08 (aromatic), 80.16 (bound CH₂O⁻), 71.54 (tertiary C), 65.33 (free CH₂OH) and**

19.12 (CH₃); ⁹⁵Mo NMR: δ 33.0; FTIR (KBr matrix, in cm⁻¹) ν(OH) 3290, 3284; ν(C=N) 1627; ν(MoO₂) 943, 882; UV/VIS (dmf): λ/nm (ε/M⁻¹ cm⁻¹) 260 (13 775), 305 (12 330) and 380 (4542).

[MoO₂(H₂L⁹)(H₂O)]·H₂O **13** (Found: C, 41.34; H, 4.20; Mo, 22.29; N, 3.13. Calc. for C₁₅H₁₉MoNO₈: C, 41.20; H, 4.35; Mo, 21.96; N, 3.20%). ¹H NMR: δ 9.44 (s, 1 H, imine), 8.28–7.15 (m, aromatic), 5.12 (t, 2 H, free CH₂OH), 4.51 (s, 2 H, CH₂O⁻) and 3.90–3.67 (m, 4 H, free CH₂OH); ¹³C NMR: δ 158.81 (imine), 160.49–111.21 (aromatic), 76.81 (bound CH₂O⁻), 74.48 (tertiary C) and 61.27 (free CH₂OH); ⁹⁵Mo NMR: δ 37.0; FTIR (KBr matrix, in cm⁻¹) ν(OH) 3383, 3228; ν(C=N) 1623; ν(MoO₂) 931, 886; UV/VIS (dmf): λ/nm (ε/M⁻¹ cm⁻¹) 261 (14 491), 304 (12 464) and 378 (4627).

[MoO₂(L_r¹)(H₂O)] **14** (Found: C, 39.02; H, 5.36; Mo, 28.62; N, 4.01. Calc. for C₁₁H₁₇MoNO₅: C, 38.94; H, 5.02; Mo, 28.31; N, 4.13%). ¹H NMR: δ 7.17–6.69 (m, aromatic), 4.22 (br, 1 H, NH), 4.02 (s, 2 H, CH₂O⁻), 3.92–3.86 (s, 2 H, CH₂N), 1.34, 1.24 (s, 6 H, CH₃); ¹³C NMR: δ 160.39–118.05 (aromatic), 83.80 (bound CH₂O⁻), 61.84 (tertiary C), 45.19 (CH₂N), 21.46, 21.07 (CH₃); ⁹⁵Mo NMR: δ 56.3; FTIR (KBr matrix, in cm⁻¹) ν(OH) 3439; ν(NH) 3228; ν(MoO₂) 922, 838; UV/VIS (dmf): λ/nm (ε/M⁻¹ cm⁻¹) 277 (5466) and 321 (2407).

[MoO₂(HL⁴)(MeOH)] **15** (Found: C, 38.71; H, 5.62; Mo, 25.83; N, 4.01. Calc. for C₁₂H₁₉MoNO₆: C, 39.03; H, 5.15; Mo, 26.00; N, 3.79%). ¹H NMR: δ 8.68 (br, 1 H, NH), 7.23–6.67 (m, aromatic), 6.39 (br, 1 H, OH), 4.29 (s, 2 H, CH₂O⁻), 3.88–3.73 (s, 2 H, CH₂N), 3.65–3.55 (m, 2 H, free CH₂OH) and 1.07 (s, 3 H, CH₃); ¹³C NMR: δ 164.72–116.26 (aromatic), 82.06 (bound CH₂O⁻), 63.30 (tertiary C), 64.98 (free CH₂OH), 42.58 (CH₂N) and 14.00 (CH₃); ⁹⁵Mo NMR: δ 80.3; FTIR (KBr matrix, in cm⁻¹) ν(OH) 3453; ν(NH) 3200; ν(MoO₂) 921, 876; UV/VIS (dmf): λ/nm (ε/M⁻¹ cm⁻¹) 260 (7565), 278 (4942) and 312 (1381).

[MoO₂(H₂L_r⁷)(H₂O)]·H₂O **16** (Found: C, 33.65; H, 4.70; Mo, 24.38; N, 3.93. Calc. for C₁₁H₁₉MoNO₈: C, 33.94; H, 4.89; Mo, 24.67; N, 3.60%). ¹H NMR: δ 8.39 (br, 1 H, NH), 7.21–6.67 (m, aromatic), 6.08, 4.96 (br, 2 H, OH), 4.39 (s, 2 H, CH₂O⁻), 4.05–3.81 (s, 2 H, CH₂N) and 3.79–3.70 (s, 2 H, free CH₂OH); ¹³C NMR: δ 164.39–116.42 (aromatic), 79.32 (bound CH₂O⁻), 66.85 (tertiary C), 62.39, 59.63 (free CH₂OH) and 43.42 (CH₂N); ⁹⁵Mo NMR: δ 81.9; FTIR (KBr matrix, in cm⁻¹) ν(OH) 3453; ν(NH) 3221; ν(MoO₂) 928, 891; UV/VIS (dmf): λ/nm (ε/M⁻¹ cm⁻¹) 259 (7700), 277 (5024) and 312 (1248).

The *cis*-dioxomolybdenum(vi) complexes were generally recrystallized either from dmsO or dmf. Complexes **5**·H₂O·dmf, **9**·dmsO, **10**·dmsO and **12**·dmf yielded crystals suitable for single-crystal X-ray analysis.

Complexes [VO(L¹)(quin)] **17**,⁹ [Hamp][VO₂L¹] **18**,^{10a} [VO(salamq)(cat)], **19**,^{11b} [VO(HL⁷)]₂, **20**,^{9,11} [VO(hnanth)(OMe)(MeOH)] **21**,^{11c} [VO₂(H₂L¹⁰)]⁻ **22**,¹⁴ [VO(tea)] **23**,¹⁵ [Mn^{IV}(H₂L⁷)₂]¹² and [Mn^{II}Mn^{III}(H₂L⁷)(O₂CMe)₄(MeOH)₂]¹³ were synthesized as reported earlier.

X-Ray crystallography

Standard procedures were used for mounting the crystals. As the crystals were found to be stable, no special protection was employed. The diffraction data were collected at 293(2) K for complex **3** on a Nicolet R3m/V, for **4**, **5**·H₂O·dmf, **9**·dmsO and **10**·dmsO on a Rigaku AFC7S and for **12**·dmf on a CAD4 diffractometer in the ω–2θ scan mode using Mo-Kα radiation (λ 0.710 73 Å). The data reduction involved all preliminary corrections. No significant decay was observed with the standard reflections. The structures were solved using SHELXS 86¹⁸ and the model was refined using SHELXTL PLUS and SHELXL 93.¹⁹ The diagrams were generated using XPMA or ZORTEP.²⁰ The hydrogen atoms were placed in fixed geometries using SHELXL. Fourier-difference syntheses were used to locate the H atoms associated with H₂O and H₃O⁺. An empirical absorp-

tion correction was made for all the data. Full-matrix least-squares refinement with anisotropic thermal parameters for all non-hydrogen atoms was used. The hydrogen atoms were treated as riding atoms with a fixed thermal parameter. In the case of **4** with a non-centrosymmetric space group the opposite hand was also refined and compared. Other details of collection and refinement are provided in Table 1.

CCDC reference number 186/999.

Bromination studies

The solution behaviour of various vanadium(v) complexes was studied in the presence of added water, HClO₄ or H₂O₂ and the reactions were monitored using UV/VIS absorption and ⁵¹V NMR spectra. For the bromination reactions, stock solutions of the complexes were prepared in 0.05 M HClO₄ in dmf solutions. The reactions were carried out after equilibrating for 10–30 min. Bromination of xylene cyanole was measured by the decrease in absorbance at 615 nm, as reported by Clague and Butler^{3c} (Δε = 6000 M⁻¹ cm⁻¹ at 0.05 M HClO₄) in the presence of KBr, H₂O₂ and vanadium(v) complexes. The order of addition of reagents was found to be critical. Control experiments were performed in the absence of V^V and/or H₂O₂ and also only in the presence of H₂L¹. Similar brominations, were attempted using MoO₂²⁺ complexes **5–7** but without success.

Transmetalation reactions

Quantitative transmetalation reactions of MoO₂²⁺ complexes **5–7**, **9**, **10** with [VO(acac)₂] or VOSO₄ were carried out in a similar manner and a typical reaction with **7** is described. Complex **7** (0.351 g, 1 mmol) was suspended in MeOH (10 cm³) [VO(acac)₂] (0.267 g, 1 mmol) or VOSO₄ (0.217, 1 mmol) added in MeOH (10 cm³) and refluxed at 50 °C for 4 h. A brown precipitate was filtered off and washed thrice in MeOH for 6 h each time and crystallized as a red-brown solid. This was identified as complex **20** based on proton NMR, FTIR and UV/VIS studies.^{9,11} However no vanadium complex could be isolated from the reaction of [MoO₂L¹] **5** (0.350 g, 1 mmol) with [VO(acac)₂] (0.267 g, 1 mmol).

Separation of VO³⁺ from a mixture of [VO(acac)₂] and [MoO₂(acac)₂]

From a mixture containing [VO(acac)₂] (0.267 g, 1 mmol) and [MoO₂(acac)₂] (0.328 g) in MeOH (25 cm³), corresponding complexes **20** and **7**, were separated one after the other after sequential addition of H₄L⁷ (1 mmol). Similar studies were also carried out using H₄L_r⁷.

Binding studies

The binding constants for H₄L⁷ and H₄L_r⁷ with VO³⁺ and MoO₂²⁺, and those of H₄L_r⁷ and H₃tea with VO³⁺, have been determined using the Hildebrand–Benesi equation.²¹ The increase in the absorbance at 522 and 474 nm was used to obtain the binding constants in the case of the reactions for H₄L⁷ and H₄L_r⁷ with vanadium species respectively, and the increase in absorbance at 411 nm was used for calculating the binding constants for Mo using H₄L⁷.

Conductivity measurements

Polyaniline was deposited on a platinum twin-wire electrode by electropolymerization from a monomer containing 0.1 M aniline in 0.5 M H₂SO₄.²² The polymerization was carried out by potentiodynamic cycling between –0.2 and +0.8 V vs. SCE using an EG&G PARC model 362 potentiostat/galvanostat. A 50 mM solution of H₄L⁷ (10 μl) was immobilized in the polyaniline matrix and the solvent was allowed to evaporate in air. The resulting sensor was subjected to various concentrations of V and Mo, prepared in pH 7.0 buffer. A current of 100 nA (at 1.33

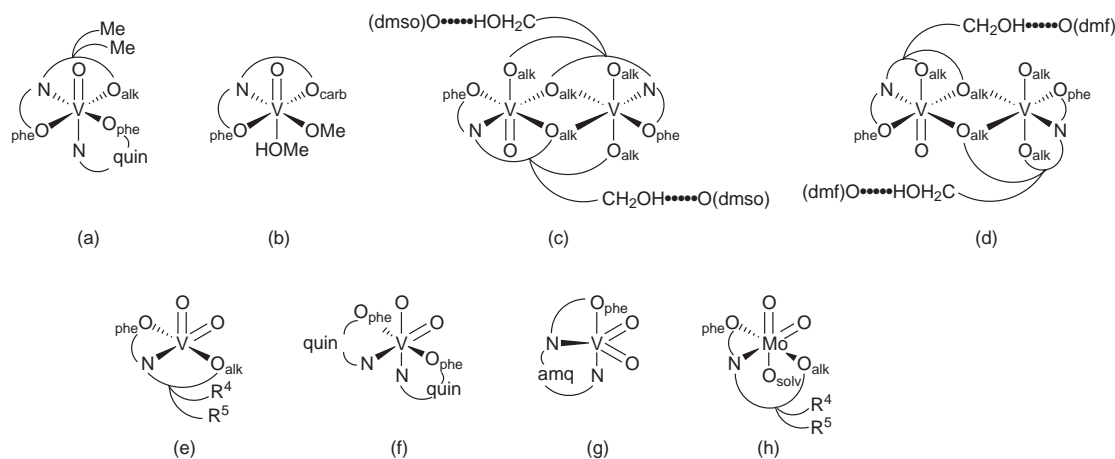


Fig. 1 Diverse core structures of oxo-vanadium(v) and -molybdenum(vi) centers based on our single-crystal X-ray studies. alk = Alkoxo, phe = phenoxo, carb = carboxylato; R⁴ = R⁵ = Me or CH₂OH e; R⁴ = Me, R⁵ = CH₂OH h

KHz) was forced through the sensor, and the in-phase voltage across the sensor was measured on an EG&G PARC model 5208 two-phase Lock-in analyser. The ratio of the in-phase voltage to the current gave the resistance. The conductance was obtained by taking the inverse of resistance assuming that it is a reasonable estimate of the conductance of the polymer film. The sensor 'response' is represented by $\Delta g/g_0$,²² where g_0 is the conductance of the sensor in buffer without the metal ion and $\Delta g = g - g_0$, where g is the small signal conductance of the sensor in the presence of the metal ion.

Results and Discussion

Synthesis

Synthetic reactions were primarily carried out using potential tri-, tetra-, and penta-dentate Schiff-base ligands possessing one, two or three CH₂OH functions respectively and their NaBH₄-reduced counterparts having a CH₂NH (amine) moiety instead of CH=N (imine). In spite of several variations, such as denticity of the ligand and/or the presence of imine or amine, the reaction always yielded mononuclear complexes of oxo-vanadium(v), and -molybdenum(vi), where the ligands acted in a tridentate manner, with an exception in the case of vanadium where a pentadentate ligand (H₄L⁷ having imine or H₄L_r⁷ having amine) resulted in tetradentate binding, with a dinuclear formation through a bridging CH₂O⁻ moiety. Even the use of a vanadium(IV) synthetic precursor yielded the formation of oxo vanadium(v) species. Reactions were also carried out in the case of vanadium using bidentate Hquin, resulting in the complex [H₃O][VO₂(quin)]₂. Thus all the synthetic reactions resulted in a variety of complexes with variations in the denticity of the ligand, geometry, co-ordination number and type as discussed below. The subtle variations in the nature of the complexes are responsible for their diverse reactivities and species recognition. The use of vanadium(v) complexes as oxidative catalysts²³ or as functional mimics of vanadium haloperoxidases (V-HPO's)^{3a,24} depends upon the reactivity of these complexes towards peroxide under acidic conditions.

Structural diversity

All our synthetic efforts resulted in the formation of complexes with different oxometal centers, such as VO³⁺, *cis*-VO₂⁺, and *cis*-MoO₂²⁺, and with different co-ordination geometries and charge types, resulting totally in eight different types of structures as shown in Fig. 1. All these structures are established based on single-crystal X-ray diffraction studies. While vanadium exhibits both five- and six-co-ordinated structures, Mo exhibited only six-co-ordinated ones. Oxovanadium(v) has shown some less common dinuclear structures, c and d, with a

centrosymmetric V₂O₂ core, and all the others were mononuclear. Instead of forming dinuclear structures, generally *cis*-MoO₂²⁺ picks up a solvent molecule to give a mononuclear complex, even when some unbound (free) CH₂OH groups are available. In all the cases the metal core geometries are highly distorted and range from trigonal bipyramidal (g) to square pyramidal (e) to octahedral.

A large number of low molecular-weight oxovanadium complexes have been reported. In addition to the oxo-metal moiety, the cores of these are essentially bound to phenoxo and imine nitrogen moieties,²⁵ and in a very few cases through carboxylate^{3a,26} and alkoxo moieties,^{15,27} exhibiting five- or six-co-ordinated monooxovanadium, dioxovanadium as a monomer and/or a weak dimer including that of Pecoraro's asymmetric V₂O₂ core,^{25c} and a dimer formed between V^{IV} and V^V. Thus the co-ordination spheres of the complexes reported by us differ from these particularly in their binding to alkoxo moieties at large. The differences lie in the type of co-ordination geometry and ligation, total charge on the species, monoxo *vs.* dioxo, monomer *vs.* dimer and in the number of alkoxo moieties bound and unbound. While on the one hand they are reflected in the solid state structures at both the molecular and lattice levels, on the other they are reflected in properties such as solubility and reactivity. Thus, the systems reported in this paper are good candidate molecules for further studies in the context of their primary co-ordination, structure, reactivity and selectivity.

Bond distances and angles of the primary co-ordination spheres of all the structures are compared in Table 2. There are expected increases in the bond distances M=O, M-O_{alk}, and M-O_{phe} on going from oxo-vanadium(v) to -molybdenum(vi) complexes. In all the *cis*-oxometal cores the nitrogen from a HC=N or H₂CNH group of the ligand occupies a near *trans* position to M=O bond. This is understandable from a plot of the M=O distances and O=M-N angles where the O=M-N angles vary between 120° and 160° among various oxo-vanadium(v) and -molybdenum(vi) complexes. Other details of these molecular structures and their lattice interactions are discussed individually.

Complex 3-2dmf. The crystal structure of 3-2dmf revealed a dinuclear octahedral, monooxovanadium(v) moiety having an inversion center (with V₂O₂ core) where H₄L_r⁷ acts in a tetradentate manner by using two of its alkoxo moieties for metal binding as shown in Fig. 2. A major structural difference between [{VO(H₂L⁸)₂]₂⁹ and 3 is the manner in which the H₄L⁸ and H₄L_r⁷ ligands bind to the metal centers. These structures displayed V₂O₂ rhombs with a non-bonded V...V distance of 3.214 Å in 3 and 3.372 Å in [{VO(H₂L⁸)₂]₂. Structure 3 exhibited marginal changes in bond lengths and angles as compared to [{VO(H₂L⁸)₂]₂ and a significant change indicating the con-

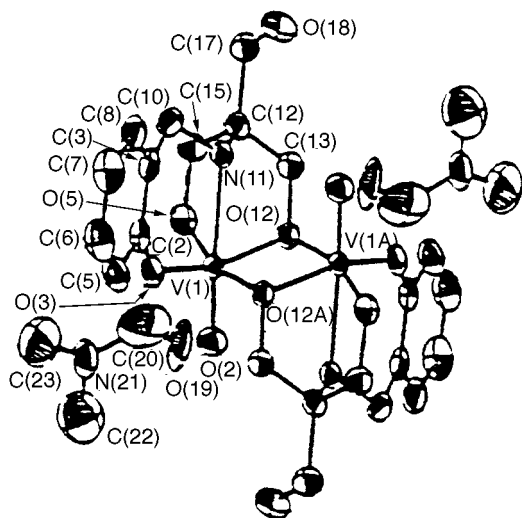


Fig. 2 Molecular structure of complex 3·2dmf showing 50% probability thermal ellipsoids

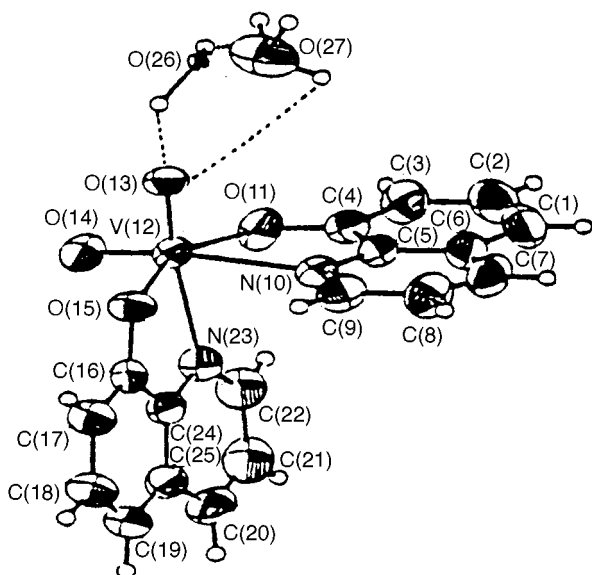


Fig. 3 Molecular structure of complex 4 showing 50% probability thermal ellipsoids

version of HC=N (1.272 Å in $[\{VO(H_2L^8)\}_2]$) to H_2CNH (1.470 Å in **3**) upon $NaBH_4$ reduction.

In the lattice of complex 3·2dmf the dmf molecules are involved in one weak C(6)–H···O(19) (3.183 Å) and one strong O(18A)–H···O(19) (2.463 Å) hydrogen-bond interaction, leading to interconnectivity of vanadium complex molecules in the lattice. An intramolecular hydrogen-bond was noticed, N(11)–H···O(18) 2.864 Å. Displaced face to face interactions of aromatic rings (offset π – π) with C···C distances ranging from 3.536 to 3.889 Å between the dinuclear units lead to self-assembly of **3** in the lattice. Such extended interactions are not seen in the lattice structure of $[\{VO(H_2L^8)\}_2]$ even though the space group of both lattices is the same ($P2_1/c$), owing to the differences in their co-ordination types.

Complex 4. The crystal structure of complex **4** showed a distorted octahedral geometry where the nitrogen atoms of both oxines are found *trans* to the oxido ligands, and the phenolic oxygens and oxo groups complete the co-ordination sphere as shown in Fig. 3. The V–O_{phe} distances of 1.963 and 1.978 Å are longer than found in the corresponding mixed-ligand complex $[VO(L^1)(quin)]^9$ (1.861 Å). The V=O distances of 1.619 and 1.630 Å are in the normal range for dioxo complexes.^{9,10} The

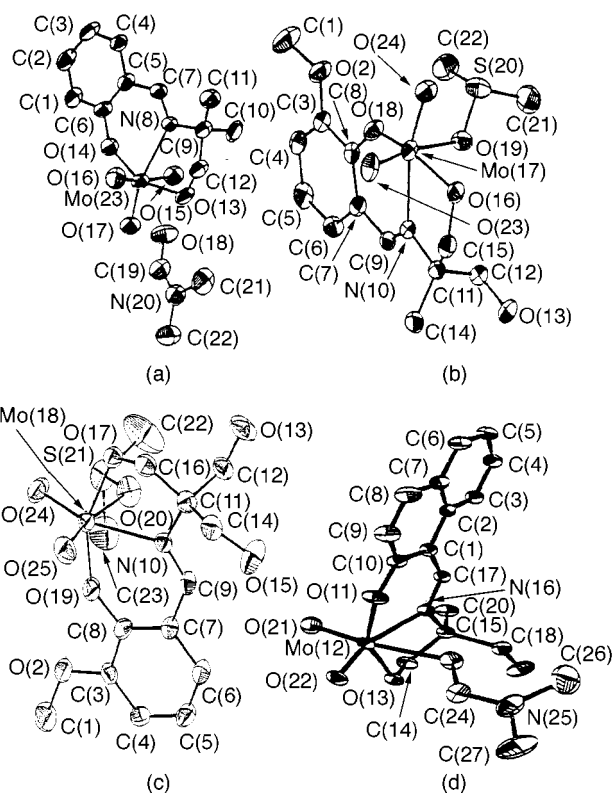


Fig. 4 Molecular structure showing 50% probability thermal ellipsoids for complexes (a) **5**, (b) **9**, (c) **10** and (d) **12**

O–V–O angle of 103.3° of the *cis*-dioxovanadium center in **4** is smaller than that found with our other complexes (105–111°).^{9,10} Three intramolecular hydrogen-bond interactions, *i.e.* O(26) (H₂O)···O(13) (V=O) 2.356, O(26) (H₂O)···O(27) (H₃O⁺) 2.300 and O(27) (H₃O⁺)···O(13) (V=O) 3.289 Å, stabilize the complex resulting in the formation of a six-membered hydrogen-bonded ring as shown in Fig. 3. The two short O···O distances indicate very strong hydrogen-bond interactions. Short O···O distances (2.29 Å) are observed relatively infrequently.²⁸

Complex **4** also showed interesting molecular packing due to self-assembly, consisting of two types of feeble intermolecular stacking interactions, *i.e.* the edge-to-face aromatic C–H··· π interactions (six in the range 3.148–4.300 Å) and the offset π ··· π interactions (aromatic C···C in the range 3.790–4.330 Å). However, a chemically similar anion to that of **4** with a bulky counter cation, NBu_4^+ , exhibited no such stacking interactions²⁹ and has a much different hydrogen-bonding pattern due to the presence of a molecular two-fold axis of symmetry.

Complexes 5, 9, 10 and 12. In the crystal structures of complexes **5, 9, 10** and **12** the Schiff-base ligands act in a dianionic tridentate manner binding through only one alkoxo O giving the Mo a distorted octahedral geometry. The molecular structures of these complexes are shown in Fig. 4. Both the Mo=O distances (1.691–1.719 Å) and the O–Mo–O angles (106.0–106.3°) are in the usual range for *cis*-MoO₂ complexes.³⁰ The imine nitrogen is *trans* to Mo=O with an average Mo–N distance of 2.281 Å, within the range observed previously (2.28–2.50 Å).³⁰ The Mo–O_{alk} distances are in the range 1.921–1.945 Å, the Mo–O_{phen} distances in the range 1.931–1.961 Å. The sixth position is occupied by a solvent molecule with the average Mo–O_{solv} (solv = H₂O or dmsO) distance of 2.346 Å. While all the ligands (irrespective of the number of CH₂OH groups) bind in a tridentate manner in molybdenum complexes **6, 9, 12**, and **7, 10, 13**, the same ligands are bound in a tetradentate manner utilizing two of their alkoxo groups in the case of oxovanadium(v) complexes, resulting in dinuclear species

Table 1 Summary of crystallographic data^a and parameters for complexes **3-2dmf**, **4**, **5**, **9**, **10** and **12**

	3	4	5	9	10	12
Molecular formula	C ₂₈ H ₄₂ N ₄ O ₁₂ V ₂	C ₁₈ H ₁₇ N ₂ O ₆ V	C ₁₄ H ₂₂ MoN ₂ O ₆	C ₁₄ H ₂₁ MoNO ₇ S	C ₁₄ H ₂₁ MoNO ₈ S	C ₁₈ H ₂₂ MoN ₂ O ₆
<i>M</i>	728.54	408.28	410.26	443.32	459.32	458.32
Crystal system	Monoclinic	Tetragonal	Monoclinic	Monoclinic	Monoclinic	Monoclinic
Space group	<i>P</i> 2 ₁ / <i>c</i>	<i>I</i> 4	<i>P</i> 2 ₁ / <i>c</i>	<i>P</i> 2 ₁ / <i>n</i>	<i>P</i> 2 ₁ / <i>n</i>	<i>P</i> 2 ₁ / <i>c</i>
<i>a</i> /Å	11.330(5)	19.931(3)	7.011(4)	14.365(7)	14.305(3)	12.922(3)
<i>b</i> /Å	12.057(6)	19.931(3)	19.446(3)	9.072(2)	9.249(2)	10.059(2)
<i>c</i> /Å	13.103(6)	8.900(3)	12.787(4)	15.332(8)	14.860(3)	15.162(6)
β/°	113.98(3)	—	95.01(3)	117.32(4)	115.38(13)	103.39(2)
<i>U</i> /Å ³	1635.4(13)	3535.7(12)	1736.6(12)	1775.2(14)	1776.3(6)	1917.2(9)
<i>Z</i>	2	8	4	4	4	4
<i>D</i> _c /g cm ⁻³	1.467	1.534	1.562	1.659	1.718	1.588
<i>F</i> (000)	756	1680	832	904	936	936
Total reflections	2235	1765	3324	3252	3818	3515
Unique reflections	2003	1754	3060	3120	3121	3358
Reflections used ^b	1698	1595	2501	2695	2751	2985
Parameters	209	260	209	218	227	246
Final <i>R</i>	0.0607	0.0507	0.0621	0.0410	0.0500	0.0348
<i>R</i> ' ^c	0.1662	0.1426	0.1950	0.1017	0.1280	0.0968

^a Data were collected using Mo-Kα radiation (λ = 0.710 69 Å) in the range θ 2–25°. ^b Reflections used are those whose *I* > 2σ(*I*). ^c A Chebychev weighting scheme was employed; *R*' = [Σw(|*F*_o| - |*F*_c|)²/Σw|*F*_o|²]^{1/2}, where *w* = [1/σ(*F*²)] + 1.00.

Table 2 Selected bond distances (Å) and angles (°) for the primary co-ordination spheres of the complexes

	3	4	5	9	10	12
M=O	1.601(4)	1.619(6), 1.630(5)	1.702(6)	1.691(4)	1.697(4)	1.697(2)
M–O _{phe}	1.834(4)	1.963(6), 1.978(6)	1.712(7)	1.706(4)	1.703(4)	1.719(2)
M–O _{alk}	1.809(4), 1.997(4)	—	1.961(6)	1.931(3)	1.955(3)	1.951(2)
M–O _{solv}	—	—	1.921(6)	1.945(3)	1.933(3)	1.941(2)
M–N	2.288(5)	2.336(6), 2.287(6)	2.354(7)	2.365(4)	2.339(4)	2.325(2)
O=M=O	—	103.3(3)	106.0(3)	106.3(2)	106.0(2)	106.0(1)
O=M–O _{phe}	100.9(2)	96.5(3), 102.3(3), 93.0(2), 101.5(3)	96.1(3)	97.5(2)	97.2(2)	98.0(1)
O=M–O _{alk}	96.5(2), 101.6(2), 95.7(2)	—	100.3(3)	98.7(2)	102.0(2)	100.4(1)
O=M–O _{solv}	—	—	98.0(2)	97.2(2)	96.7(2)	97.5(1)
O=M–N	172.6(2)	90.2(3), 163.8(3), 90.4(3), 165.3(3)	98.0(3)	99.9(2)	97.3(2)	97.9(1)
O _{phe} –M–O _{alk}	103.1(2), 152.5(2), 88.3(2)	—	81.6(3)	85.0(2)	85.4(2)	82.4(1)
O _{phe} –M–O _{solv}	—	—	171.6(3)	168.5(2)	168.5(2)	170.5(1)
O _{phe} –M–N	86.1(2)	75.1(2), 84.8(3), 90.2(3), 165.3(3)	94.6(3)	92.4(2)	93.2(2)	92.6(1)
O _{alk} –M–O _{solv}	—	—	158.8(3)	160.9(2)	159.8(2)	161.0(1)
O _{alk} –M–N	79.1(2), 72.5(2), 87.2(2)	—	152.8(3)	152.0(1)	152.1(12)	151.8(1)
O _{solv} –M–N	—	—	78.8(2)	78.5(1)	78.6(2)	78.4(1)
O _{phe} –M–O _{phe}	—	153.0(2)	81.8(2)	81.2(1)	81.5(1)	80.6(1)
N–M–N	—	77.2(2)	—	—	—	—
O _{alk} –M–O _{alk}	89.8(2), 161.4(2), 73.9(2)	—	84.2(2)	82.5(1)	82.5(1)	82.1(1)
O _{phe} –M–O _{phe}	—	—	74.0(2)	74.4(1)	74.1(1)	75.5(1)
N–M–N	—	—	78.2(2)	76.4(1)	75.7(1)	78.1(1)

N = Nitrogen of CH₂NH or CH=N or Hquin.

bridged through alkoxo moieties.⁹ However in the presence of an excess of KOH, mononuclear *cis*-dioxovanadium(v) complexes were generated where the ligand acts only in a tridentate manner.⁹ However, the same ligands acted in a tetradentate manner in [Cu₂Mo₂O₄L₂(OMe)₂]³¹ and tridentate in [CuMo₃O₈L⁴(bipy)₂],³² [Mn^{IV}(H₂L⁷)₂],¹² and [Mn^{II}Mn₂^{III}L⁷(O₂CMe)₄(MeOH)₂].¹³

An interesting feature of dmsO reductase is the Mo–O bond distance of 1.92 Å observed by EXAFS.⁷ Based on the single-crystal data of small molecules reported in this paper and in the literature,³⁰ it is tempting to interpret this distance as the one derived from a Mo–O_{alk} bond *cis* to Mo=O. The recent single-crystal analysis of dmsO reductase (reduced form) showed a Mo=O distance of 1.6 Å and a Mo–O_{ser} distance of 2.0 Å, in agreement with those predicted based on alkoxo-bound oxomolybdenum complexes. While the oxidized enzyme possesses

cis-MoO₂²⁺ and serine ⁻O⁻, the reduced form possesses an Mo=O, serine ⁻O⁻ and dmsO.^{8b,c} However the metal core structure based on the earlier studies of dmsO reductase obtained from *Rhodobacter sphaeroides* was found to be different.^{8a}

FTIR and UV/VIS studies

The FTIR data are consistent with the presence as well as the binding of the H₂CNH unit in the vanadium complexes **1–3**. The presence of unbound OH groups in **3** is delineated through the ν(OH) region. The ν(V=O) region is consistent^{9–11} with the *cis*-dioxo nature of **1** and **4**, and monoxo in the case of **2** and **3**. No free ν(OH) bands were seen for complex **2** indicating the involvement of both alkoxo groups in metal binding through deprotonation. Pale yellow complexes **1** and **4** showed LMCT and intraligand transitions consistent with the dioxo-

vanadium(v) complexes. Complex **3**, on the other hand, is deep red-brown and showed absorption bands in the visible region, with a low energy band at 474 nm ($p_{\pi} \rightarrow d$ charge transfer) assignable to either VO^{3+} -bound phenolates or a 'bare' vanadium(v) form.³³ However, based on the observation of $\nu(\text{V}=\text{O})$ from FTIR and the presence of a VO^{3+} center in the structure of complex **3**, the second possibility is ruled out.

The two bands observed for ν_{asym} and ν_{sym} vibrations of the $\text{O}=\text{Mo}=\text{O}$ moiety of complexes **5–16** are consistent with a *cis*- MoO_2 structure. In the region $3000\text{--}3400\text{ cm}^{-1}$ complexes **5–13** showed a broad band accounting for unbound CH_2OH and/or water. Co-ordination of the imine center through nitrogen is also reflected in the low-frequency shift of the $\nu(\text{C}=\text{N})$ by about $15\text{--}25\text{ cm}^{-1}$. The FTIR spectra of complexes **14–16** reveal the disappearance of $\nu(\text{C}=\text{N})$ as expected, since these complexes are synthesized using reduced Schiff bases L_r . A plot of $\nu_{\text{Mo}=\text{O}}$ vs. $\text{Mo}=\text{O}$ bond distance was approximately linear for a number of oxomolybdenum complexes (SUP 57388) with a slope of 17 cm^{-1} per 0.01 \AA . A similar plot in case of oxovanadium(v) complexes showed a slope of 14 cm^{-1} per 0.01 \AA .⁹ The electronic spectra of complexes **5–16** recorded in dmf exhibited LMCT bands in the region $304\text{--}381\text{ nm}$ and $\pi \rightarrow \pi^*$ transitions around $266 \pm 6\text{ nm}$. The LMCT transitions showed a near linear correlation with respect to ^{95}Mo NMR chemical shifts (SUP 57388) as explained in the NMR section. Both the FTIR and UV/VIS spectra are in good agreement with those reported for several *cis*- MoO_2^{2+} complexes.³⁰

NMR studies

Both ^1H and ^{13}C NMR spectra of complexes **1** and **3** are consistent with the binding of a reduced Schiff base (H_2CNH). Complex **1** showed a downfield shift of about 9 ppm in the ^{13}C NMR spectrum for the bound CH_2O^- similar to that observed in the case of Schiff-base complexes of the type $[\text{VO}_2\text{L}]^-$ (where $L = L^1, L^2$ or L^3).^{10a} Both the ^1H and ^{13}C NMR spectra of **3** are consistent with two bound CH_2O^- groups and one unbound CH_2OH group. The resonances were assigned based on COSY and DEPT-135 NMR experiments.

The magnitude of deshielding in NMR spectroscopy is found to be inversely proportional to the energy of the LMCT. A plot of the wavelength of the LMCT transition vs. the ^{51}V NMR chemical shift was approximately linear (SUP 57388) with a slope of 10 ppm per 10 nm. However, for the vanadium(v) complexes without a coligand (such as catecholate or hydroximate) an approximately linear plot with a negative slope of $-2\text{ ppm per } 10\text{ nm}$ (SUP 57388) was observed. As Pecoraro and co-workers suggested earlier,³⁴ our observations rule out the involvement of non-innocent coligands, such as catecholate or hydroximate, in the co-ordination sphere of V^{V} in case of the enzyme V-HPO.

Both ^1H and ^{13}C NMR spectra of the molybdenum complexes **5–16** are indicative of binding of the corresponding ligands through a phenoxo, alkoxo and imine group, leaving any additional CH_2OH groups unbound. Proton NMR spectra in the CH_2 region of bound CH_2O^- exhibited either a singlet or diastereotopic multiplet depending upon the symmetric or non-symmetric disposition of substituents on the neighbouring tertiary carbon center. Thus for $(\text{R}^4\text{R}^5)\text{CCH}_2\text{O}^-$ a singlet was seen when $\text{R}^4 = \text{R}^5 = \text{Me}$ or CH_2OH , and a diastereotopic multiplet was observed for the other non-symmetric combination (where R^4 and R^5 are different). This behaviour is seen in both oxovanadium(v) and -molybdenum(vi) complexes. Representative spectra in the CH_2 region are shown in Fig. 5 for oxomolybdenum(vi) complexes. The CH_2 region indeed provides a signature to differentiate a mononuclear from a dinuclear complex, where in the latter case a second CH_2O^- function is bridging as observed in complexes possessing V_2O_2 rhombs, *i.e.* **3** and **20**. The ^{51}V NMR chemical shifts followed an inverse electro-negativity relation.³⁵ The ^{95}Mo chemical shifts of alkoxo-bound

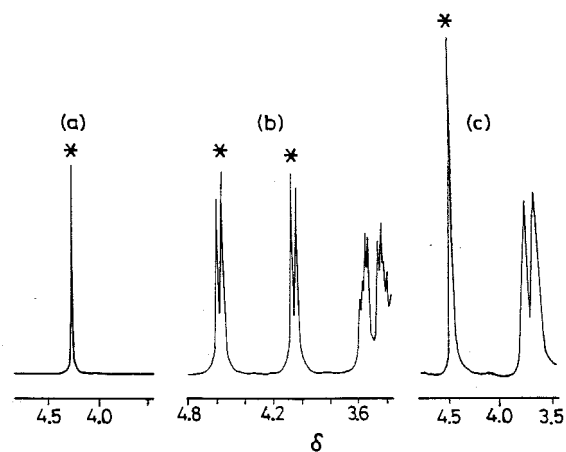


Fig. 5 Proton NMR spectra of oxomolybdenum(vi) complexes in the CH_2 region: (a) **5**, (b) **6** and (c) **7**, possessing one, two and three CH_2OH groups (H_2L^1 , H_3L^4 and H_4L^7) respectively. Asterisked peaks are from the bound CH_2 group

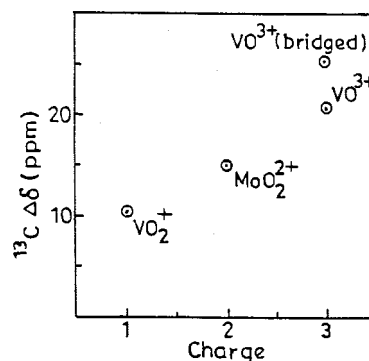


Fig. 6 Plot of charge on oxometal species vs. ^{13}C $\Delta\delta$ CIS of the bound CH_2O^- function

MoO_2^{2+} complexes **5–16** (δ 31 to 82) are comparatively more deshielded with respect to seven-co-ordinate MoO^{4+} (δ -55 to $+5$)³⁶ and lie in the range observed for six-co-ordinate MoO_2^{2+} complexes (δ -219 to $+58$).³⁷ A plot of the wavelength for the LMCT vs. ^{95}Mo NMR shifts for a set of *cis*- MoO_2^{2+} complexes was approximately linear with a positive slope of 2 ppm per 10 nm (SUP 57388). In ^{13}C NMR spectra the co-ordination induced shifts ($\text{CIS} = \delta_{\text{complex}} - \delta_{\text{ligand}}$ ppm) for the bound alkoxo group for the complexes of oxo-vanadium(v) and -molybdenum(vi) are dependent on the charge of the oxometal species (1+, 2+ or 3+) and also on the nature of the alkoxo group binding, terminal or bridging as shown in Fig. 6. The higher the charge on the oxometal species the larger is the CIS and the shift is greater for a bridging than for a terminal group, as in case of **3** or **20** where the dinuclear species involves a V_2O_2 core.

Cyclic voltammetry (CV) studies

Complex **1** with a H_2CNH group exhibited a reversible electrochemical response with E_i -471 mV at scan speeds, $\nu \leq 100\text{ mV s}^{-1}$. The E_p^c of **1** is higher when compared to the corresponding Schiff-base counterpart, $[\text{Hamp}][\text{VO}_2\text{L}^1]$ ($E_i = -64\text{ mV}$).¹⁰ Complex **3** also with a H_2CNH group displayed two CV responses with E_i -317 (reversible, $\nu \geq 200\text{ mV s}^{-1}$) and -625 mV (reversible, $\nu = 50$ to 200 mV s^{-1}) respectively, whereas the complex of its corresponding Schiff-base counterpart, **20**, exhibited a response at -419 mV .

Complexes **5–16** showed only one major reduction peak in the range -0.84 to -1.31 V in dmf at a platinum working electrode. In case of **5** and **10–13** the oxidation peak appears in the range -0.412 to -0.771 V . Detailed electrochemical studies indicated that the present set of *cis*- MoO_2^{2+} alkoxo complexes

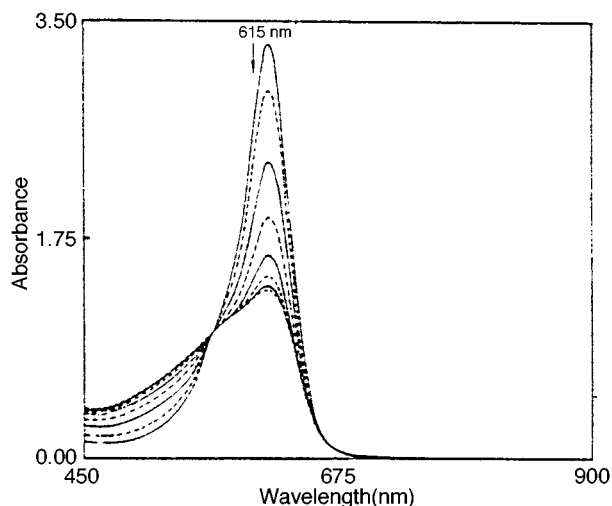


Fig. 7 Absorption spectra recorded upon bromination of xylene cyanole by *cis*-VO₂⁺ generated from a mixture of complex **17** + H₂O₂ + HClO₄ + NEt₄Br as a function of time over a period of 30 min

are electrochemically irreversible, though quasi-reversibility is observed at higher scan speeds in some cases. The E_p^c of the Mo^{VI}-Mo^V couple is low with H₂L¹, H₂L², H₂L³ (**5**, **8**, **11**) and high with the H₃L⁴, H₃L⁵, H₃L⁶ (**6**, **9**, **12**) series of complexes, and usually the 3-OMe substituted complexes have the lowest values in each set. Our results are in agreement with those for alkoxy-bound molybdenum(vi) complexes in the literature where the reduction potential (−1.13 to −1.89 V) is dependent upon the number of alkoxy groups bound to the Mo.³⁸ Such a trend has also been demonstrated in the case of alkoxy-bound vanadium complexes.⁹ However, oxomolybdenum(vi) complexes generally exhibit more negative reduction potentials as compared to those of corresponding vanadium(v) complexes as expected, indicating the fact that higher oxidation states are more stable with heavier elements.

Bromination studies

A broad absorption band in the range 300–340 nm was observed upon addition of H₂O₂ to an acidic (0.05 M HClO₄) solution of an oxovanadium(v) complex in dmf, indicating the formation of an oxoperoxovanadium(v) species. This was observed for all the complexes studied (**1**, **3**, **4**, **17–21** and **23**). The reactions were also monitored by ⁵¹V NMR spectroscopy. Addition of KBr showed a new peak at δ −560 ± 10 in the ⁵¹V NMR spectra which is assignable to a 'V–OBr' rather than a 'V–Br' species. If 'V–Br' species were formed the signals would have appeared over a large downfield region, *i.e.* δ −200 to −300, based on the inverse electronegativity principle.^{11,35} However, no such peaks were observed under these conditions. In the case of complex **4** an equilibrium mixture of *cis*-VO₂⁺, [VO₂(quin)₂][−], VO(O₂)⁺ (monoperoxo) and VO(O₂)₂[−] (diperoxo) has been identified through ⁵¹V NMR signals observed at δ −483, −521, −550 and −654 in a 2 : 1 : 2 : 2 intensity ratio. The peak at δ −521 corresponds to undissociated **4**. However, in case of the other vanadium(v) complexes, **1**, **3**, **17–21** and **23**, their regeneration does not take place, owing to cleavage or disintegration of the ligand under highly acidic conditions. A series of oxoperoxovanadium(v) complexes has been shown to have halogenation activity against phenol red by Pecoraro's group.²⁴

After sufficient equilibration of the complexes in a HClO₄-dmf mixture (10–30 min, optimized based on absorption studies), the bromination of xylene cyanole was monitored by following the decrease in the intensity of the absorption band at 615 nm (Fig. 7). Control experiments performed without the vanadium complex, and/or H₂O₂, or only in the presence of the Schiff base, H₂L¹, showed only initial bromination of xylene

cyanole to ≤5%, but the reaction did not proceed further. Also the order of addition of the reagents was found to be important. The order is as follows: sufficiently incubated complex in acid (to generate the *cis*-VO₂⁺), followed by hydrogen peroxide (to generate the mono- and di-peroxo complex),²⁴ followed by the substrate, xylene cyanole, and finally the bromide source (KBr or NEt₄Br). Under similar experimental conditions (mole ratio of substrate:vanadium complex:H₂O₂ is 45:1:20) complex **4** takes 6 min to brominate xylene cyanole while **1**, **3**, **17–21** and **23** take 120 min to achieve bromination to the same extent. Thus the brominating capacity depends upon the nature of the vanadium complex. Based on the vanadium complex to substrate ratio of 1:45, it can be proposed that these reactions are catalytic in nature, with a turnover for **4** (315 mol product per mol complex per h) being 20 times greater than that for the other complexes. In contrast to the VO₂⁺-mediated bromination reactions in 0.05 M HClO₄-dmf, V-BrPO functions optimally at pH ≈ 6.5 and at a rate 10⁴ times higher.³⁹ It looks possible that the protein undergoes rapid peroxidative halogenation probably by stabilizing the VO₂⁺ moiety through secondary interactions. Such secondary interactions were found in the crystal structure of azide-modified vanadium chloroperoxidase,⁴⁰ and hence may act as a guideline for the design of model molecules. Similar bromination reactions were also attempted with the molybdenum complexes **5–7**, but without success.

Recognition of VO³⁺ over MoO₂²⁺ species

Qualitative recognition and quantitative separation of VO³⁺ species from MoO₂²⁺ was addressed using a.c. conductivity measurements and transmetallation studies. The latter are supported by the binding studies.

Transmetallation reactions. In UV/VIS studies of a 1:1 mixture of molybdenum complex **7** and [VO(acac)₂] the band corresponding to **7** at 344 nm decreased in intensity and finally disappeared. A clear-cut isosbestic point was observed at 290 nm indicating a 1:1 equilibrium (SUP 57388). The final absorption and ⁵¹V NMR spectra are identical with those of an authentic dinuclear vanadium complex, **20**. This reaction was also monitored by ⁵¹V NMR spectroscopy. Similar transmetallation reactions between **7** and [VO(OEt)₃], VOSO₄, NH₄VO₃ or Na₃VO₄ resulted in the formation of **20**, indicating that the type of vanadium precursor used in the reaction has no effect on the final product formed. Addition of [VO(acac)₂] to molybdenum complex **6** having one free CH₂OH group yielded the corresponding VO³⁺ dimer,⁹ [{VO(L⁴)₂]₂. On the other hand, when [VO(acac)₂] was added to molybdenum complex **5** having no unbound CH₂OH group no transmetallation occurred. Thus the studies suggest that the presence of at least one unbound CH₂OH group is essential for transmetallation. Addition of VOSO₄ or [VO(acac)₂] to **16**, a molybdenum complex possessing a H₂CNH group, also led to transmetallation and the corresponding VO³⁺ dimer **3** was isolated, suggesting that the reduction of HC=N to H₂CNH does not alter the selectivity of the molecule towards VO³⁺. However, the reaction of dinuclear vanadium complex **20** with [MoO₂(acac)₂] did not show any transmetallation.

Separation of VO³⁺ species from a mixture of [VO(acac)₂] and [MoO₂(acac)₂] through selective complexation. Addition of H₄L⁷ to a mixture of [VO(acac)₂] and [MoO₂(acac)₂] (1 mmol each) in MeOH led to the isolation of the corresponding dinuclear vanadium complex **20** in the first step (first addition of the ligand) and corresponding molybdenum complex **7** in the second step of the addition of the ligand. Quantitative separations were performed. Similar quantitative separations were possible even with the use of H₄L⁷ having a CH₂NH moiety in place of CH=N. Owing to the dinuclear formation, the number of chelate rings in the vanadium(v) complex **3** is six (plus one

V₂O₅ rhomb), while it is just two in the case of the molybdenum(vi) complex **7**, thus providing a chelate stability to the vanadium(v) complex. The preferential chelation of H₄L⁷ or H₄L_r⁷ is addressed through binding studies in relation with molecules possessing similar binding motifs, such as H₃tea or H₄L¹⁰.

The binding constants for H₄L⁷ with V and Mo have been determined using the Benesi–Hildebrand equation²¹ and found to be 110 ± 2 M⁻¹ and 12 ± 1 M⁻¹ respectively, explaining the preference of H₄L⁷ to bind to V over Mo. Similarly the binding constants for H₄L_r⁷ with V and Mo were found to be 103 ± 2 and 10 ± 1 M⁻¹ respectively, a value which is comparable to that of H₄L⁷. The binding constant of H₃L⁷ (having three CH₂OH groups) with V was found to be very low, *i.e.* 0.25 ± 0.05 M⁻¹. Addition of H₄L⁷ to complex **23** (of tea) led to a very rapid conversion and isolation of **20**. The binding constant of H₄L¹⁰ with V could not be determined due to very low association. Though the formation of complex **22** (of H₄L¹⁰) in water is identified based on ⁵¹V NMR studies,¹⁴ it could not be isolated in the solid state. The ligand H₄L¹⁰ acts as a dibasic tridentate manner binding V through carboxylate oxygen, amino N and one alkoxo O. Addition of H₄L⁷ to **22** led to rapid transligation with the formation of **20** in quantitative yields. Therefore, the presence of CH₂OH groups alone (as in the case of H₃tea or H₄L¹⁰) cannot ensure selectivity towards VO³⁺ species due to their very low association constants. The solubility of vanadium complex **20** is much less than that of the molybdenum complex, **7**. Thus, in order to explain the experimentally observed results of the separation of individual oxometal species from their mixtures, both the stability and the solubility of the final products need to be considered.

A.c. conductivity measurements. Results of a.c. conductivity studies indicated a decrease in the polyaniline conductivity with increase in the concentration of the metal ion due to the change in the chemical potential of the microenvironment of the polymer²² upon metal-ion binding. The sensor response is represented by a normalized quantity, $-\Delta g/g_0$. The sensor is subjected to both V^V and Mo^{VI} independently and the results showed a linear relation between $-\Delta g/g_0$ and the concentration of the metal species, with a slope (sensitivity) of 145 mM⁻¹ for V and 0.05 mM⁻¹ for Mo, indicating a 2900-fold higher sensitivity for V as compared to that of Mo [Fig. 8(a)]. A plot of the ratio of responses of V to Mo vs. metal-ion concentration [Fig. 8(b)] suggests the possible utility of H₄L⁷ for detection of V in the presence of Mo, at concentrations >10 μM and thus H₄L⁷ acts as a metal receptor for VO³⁺ species. The selective recognition of VO³⁺ by H₄L⁷ and H₄L_r⁷ is indeed interesting in the context of the selective recognition and extraction of vanadium from sea-water by sea squirts where the concentration ratio of V to Mo is 1:5. Thus H₄L⁷ and H₄L_r⁷ show very high 'vanadophilicity'.

Conclusion

This study has effectively demonstrated the synthesis, structural diversity, reactivity, and selective oxometal recognition of new alkoxo-bound oxo-vanadium(v) and molybdenum(vi) complexes. Several interesting correlations have been drawn based on the spectral and structural data. A few relevant conclusions are as follows.

(1) Synthesis of a large variety of mono- and/or di-nuclear VO³⁺ and mononuclear *cis*-VO₂⁺ and *cis*-MoO₂²⁺ centers using alkoxo-rich ligands resulted in new complexes with eight different oxometal cores (Fig. 1). Independent of the number of CH₂OH groups present in the ligand or its denticity, only one such group binds to the *cis* MoO₂ center to give a mononuclear complex (**5–16**; co-ordinative saturation is achieved by a solvent molecule) whereas the dinuclear oxovanadium(v) complexes (**3** and **20**) are obtained involving two bound CH₂OH groups.

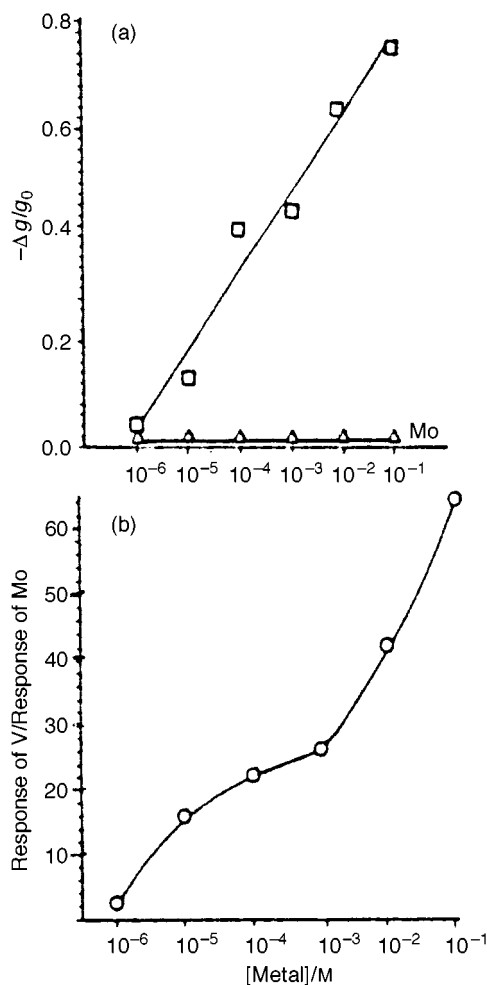


Fig. 8 (a) Response of a H₄L⁷-based molecular sensor for V^V and Mo^{VI} in phosphate buffer at pH 7.0 as a function of metal-ion concentration. (b) Ratio of the responses of V^V to Mo^{VI} as a function of metal-ion concentration

Subtle differences generated by reducing the HC=N (Schiff base) to H₂CNH (Mannich base) as in H₄L⁷ to H₄L_r⁷ result in a major change in the co-ordination geometry (Fig. 2) as well as in the lattice structure. Interesting structural interactions have been noted in the crystal lattice of these complexes, *e.g.* Fig. 3. The metric parameters of all these oxo-vanadium(v) and -molybdenum(vi) structures have shown extensive trends and correlations indicating the crystallographic accuracy.

(2) The average bond lengths of Mo=O (two such) (1.697 and 1.710 Å) and Mo–O_{alk} (1.935 Å) obtained based on our structures (**5**, **9**, **10** and **12**), together with the EXAFS and crystal structure data for dmsO reductase, support the presence of a MoO₂ center bound to serine OH in a *cis* fashion to the M=O bonds in the enzyme. On the other hand, based on the metric data obtained with the VO₂⁺ alkoxo-bound complexes, it is possible to rule out the presence of a serine OH moiety in the co-ordination sphere of the enzyme bromoperoxidase. Further, based on the LMCT transitions found in the visible region, the presence of VO³⁺ with a phenoxo moiety can also be ruled out, for the enzyme bromoperoxidase.

(3) A nice correlation has been found between the charge present on the metal core and the shift in the δ of bound CH₂O⁻ as shown in Fig. 6. A number of correlations have been established between the spectral and structural data including $\nu(M=O)$ vs. M=O distance, $\delta(^{51}V)$ (or ^{95}Mo) vs. LMCT position, O–V–O angles vs. O···O bite distance. Proton NMR spectra in the region of the bound CH₂ group have characteristic patterns differentiating mononuclear from dinuclear complexes. Based on redox potentials, it is possible to conclude

that V^V favor alkoxide donor groups over carboxylate ones and the latter favor vanadium(IV) centers. As there is no redox observed in the enzyme bromoperoxidase during catalysis, the present study suggests alkoxo rather than carboxylate binding in the enzyme. It is understandable that the reduction of V^V in these complexes is rather easy compared to that of Mo^{VI}, based on the stabilities of higher oxidation states of the heavier elements.

(4) While the Schiff-base complexes of oxovanadium(V) (**1**, **4** and **20**) possessing a HC=N moiety were found to be stable, that corresponding to the Mannich base (with H₂CNH) **3** was susceptible to hydrolysis. The reactivity of H₂O₂ has been enhanced in the presence of acid in case of oxovanadium(V) complexes.

(5) Among the oxovanadium(V) complexes (**1**, **3**, **4**, **17–21**) used in bromination reactions using phenol red or xylene cyanole as substrate under acidic conditions and with an excess H₂O₂ and NEt₄Br, **4** showed highest activity with a catalytic turnover of about 315 mol product per mol of complex per h. The presence of *cis*-VO₂⁺ and peroxo-bound VO₂ is shown to be responsible for the reactivity and the present studies eliminate the direct attack of Br⁻ at the metal ion. All the results were compared with studies of NH₄VO₃ under similar experimental conditions.

(6) The compounds H₄L⁷ and H₄L_r⁷ show specific recognition and selective complexation for VO³⁺ over MoO₂²⁺ according to studies based on quantitative separation, transmetallation, binding constants and a.c. conductivity measurements in a doped polyaniline system. This result is expected to throw light on the selective extraction of vanadium by ascidians from sea-water.

Acknowledgements

A. S. thanks the Department of Atomic Energy, India for the award of a Dr. K. S. Krishnan Research Fellowship, C. P. R. the Department of Science and Technology, Board of Research in Nuclear Sciences, India, J. S. P. the Department of Science and Technology, for funding and E. K. the Academy of Finland for support. We are grateful to Mr. R. Kaupinnen, University of Jyväskylä, Ms. S. Sukeerthi and Professor A. Q. Contractor, Indian Institute of Technology (IIT), Bombay for experimental help, Dr. P. Ghosh and Professor A. Chakravorty, Indian Association for Cultivation of Science, Calcutta, for collecting the crystal data for complex **3**, and the Regional Sophisticated Instrumentation Center, IIT, Bombay for spectral data. We thank the referees for their valuable suggestions.

References

- 1 E. Bayer, *Metal Ions In Biological Systems*, eds. H. Sigel and A. Sigel, Marcel Dekker, New York, 1995, vol. 31, p. 407; K. Raymond, *Top. Curr. Chem.*, 1984, **123**, 49.
- 2 H. Vilter, *Phytochemistry*, 1984, **23**, 1387; E. de Boer and R. Wever, *J. Biol. Chem.*, 1988, **263**, 12 326; R. Hille, *Chem. Rev.*, 1996, **96**, 2757.
- 3 (a) M. J. Clague and A. Butler, *Inorg. Chem.*, 1993, **32**, 4754; (b) D. Rehder, *Angew. Chem., Int. Ed. Engl.*, 1991, **30**, 148; (c) A. Butler and C. J. Carrano, *Coord. Chem. Rev.*, 1991, **109**, 61.
- 4 M. J. Clague and A. Butler, *J. Am. Chem. Soc.*, 1995, **117**, 3475.
- 5 M. J. Smith, D. Kim, B. Horenstein, K. Nakanishi and K. Kustin, *Acc. Chem. Res.*, 1991, **24**, 177; M. J. Smith, D. E. Ryan, K. Nakanishi, P. Frank and K. O. Hodgson, *Metal Ions In Biological Systems*, eds. H. Sigel and A. Sigel, Marcel Dekker, New York, 1995, vol. 31, p. 423.
- 6 J. M. Arber, E. de Boer, C. D. Garner, S. S. Hasnain and R. Wever, *Biochemistry*, 1989, **28**, 7968.
- 7 G. M. George, J. Hilton and K. V. Rajagopalan, *J. Am. Chem. Soc.*, 1996, **118**, 1113.
- 8 (a) H. Schindelin, C. Kisker, J. Hilton, K. V. Rajagopalan and D. C. Rees, *Science*, 1996, **272**, 1615; (b) A. S. McAlpine, A. G. McEwan, A. L. Shaw and S. Bailey, *J. Biol. Inorg. Chem.*, 1997, **2**, 690; (c) A. S. McAlpine, A. G. McEwan and S. Bailey, *J. Mol. Biol.*, 1998, **275**, 613.
- 9 G. Asgedom, A. Sreedhara, J. Kivikoski, J. Valkonen, E. Kolehmainen and C. P. Rao, *Inorg. Chem.*, 1996, **35**, 5674.
- 10 (a) G. Asgedom, A. Sreedhara, J. Kivikoski, J. Valkonen and C. P. Rao, *J. Chem. Soc., Dalton Trans.*, 1995, 2459; (b) G. Asgedom, A. Sreedhara, J. Kivikoski, E. Kolehmainen and C. P. Rao, *J. Chem. Soc., Dalton Trans.*, 1996, 93.
- 11 (a) G. Asgedom, A. Sreedhara and C. P. Rao, *Polyhedron*, 1995, **14**, 1873; (b) G. Asgedom, A. Sreedhara, C. P. Rao and E. Kolehmainen, *Polyhedron*, 1996, **15**, 3731; (c) G. Asgedom, A. Sreedhara, J. Kivikoski and C. P. Rao, *Polyhedron*, 1997, **16**, 643.
- 12 D. P. Kessissoglou, W. M. Butler and V. L. Pecoraro, *J. Chem. Soc., Chem. Commun.*, 1986, 1253.
- 13 D. P. Kessissoglou, M. L. Kirk, M. S. Lah, X. Li, C. Raptopoulou, W. Hatfield and V. L. Pecoraro, *Inorg. Chem.*, 1992, **31**, 5424.
- 14 D. C. Crans, P. M. Ehde, P. K. Shin and L. Pettersson, *J. Am. Chem. Soc.*, 1991, **113**, 3728.
- 15 D. C. Crans, H. Chen, O. P. Anderson and M. M. Miller, *J. Am. Chem. Soc.*, (a) 1993, **115**, 6769; (b) 1994, **116**, 1305.
- 16 R. A. Rowe and M. E. Jones, *Inorg. Synth.*, 1957, 114.
- 17 M. C. Chakravorti and D. Bandopadhyay, *Inorg. Synth.*, 1992, **29**, 130.
- 18 G. M. Sheldrick, SHELXS 86, Program for the solution of crystal structures, University of Göttingen, 1986.
- 19 G. M. Sheldrick, SHELXL 93, Program for the Refinement of Crystal Structures, University of Göttingen, 1993.
- 20 L. Zsoenai, XPMA/ZORTEP, University of Heidelberg, 1993.
- 21 H. Benesi and J. H. Hildebrand, *J. Am. Chem. Soc.*, 1949, **71**, 2703.
- 22 H. Sangodkar, S. Sukeerthi, R. S. Srinivasa, R. Lal and A. Q. Contractor, *Anal. Chem.*, 1996, **68**, 779.
- 23 K. Nakajima, M. Kojima and J. Fujita, *Bull. Chem. Soc. Jpn.*, 1990, **63**, 2620; D. Rehder, *Metal Ions in Biological Systems*, eds. H. Sigel and A. Sigel, Marcel Dekker, New York, 1995, vol. 31, p. 1.
- 24 G. J. Colpas, B. J. Hamstra, J. W. Kampf and V. L. Pecoraro, *J. Am. Chem. Soc.*, 1994, **116**, 3627; 1996, **118**, 3469.
- 25 (a) J. A. Bonadies, W. M. Butler, V. L. Pecoraro and C. J. Carrano, *Inorg. Chem.*, 1987, **26**, 1218; (b) K. Li, M. S. Lah and V. L. Pecoraro, *Inorg. Chem.*, 1988, **27**, 4657; (c) C. J. Carrano, C. M. Nunn, R. Quan, J. A. Bonadies and V. L. Pecoraro, *Inorg. Chem.*, 1990, **29**, 944; (d) L. M. Mokry and C. J. Carrano, *Inorg. Chem.*, 1993, **32**, 6119; (e) J. Grigg, D. Collison, C. D. Garner, M. Helliwell, P. A. Tasker and J. M. Thorpe, *J. Chem. Soc., Chem. Commun.*, 1993, 1807.
- 26 J. Costa Pessoa, J. A. L. Silva, A. L. Vieira, L. Vilas-Boas, P. O'Brien and P. Thornton, *J. Chem. Soc., Dalton Trans.*, 1992, 1745.
- 27 J. C. Dutton, K. S. Murray and E. R. T. Tiekink, *Inorg. Chim. Acta*, 1989, **166**, 5.
- 28 K. Abu-Dari, K. N. Raymond and D. P. Freyberg, *J. Am. Chem. Soc.*, 1979, **101**, 3688.
- 29 A. Giacomelli, C. Floriani, A. O. D. S. Durate, A. Villa Chiesii and C. Guastini, *Inorg. Chem.*, 1982, **21**, 3310.
- 30 J. H. Enemark and C. G. Young, *Adv. Inorg. Chem.*, 1993, **40**, 1 and refs. therein; H. R. Holm, *Chem. Rev.*, 1987, **87**, 1401.
- 31 D. P. Kessissoglou, C. P. Raptopoulou, E. G. Bakalbassis, A. Terzis and J. Mrozinski, *Inorg. Chem.*, 1992, **31**, 4339.
- 32 A. N. Papadopoulos, A. G. Hatzidimitriou, A. Gourdon and D. P. Kessissoglou, *Inorg. Chem.*, 1994, **33**, 2073.
- 33 S. Holmes and C. J. Carrano, *Inorg. Chem.*, 1991, **30**, 1231.
- 34 C. R. Cornman, G. J. Colpas, J. D. Hoeschele, J. Kampf and V. L. Pecoraro, *J. Am. Chem. Soc.*, 1992, **114**, 9925.
- 35 D. Rehder, C. Weidemann, A. Duch and W. Priebsch, *Inorg. Chem.*, 1988, **27**, 584; V. Vergopolous, W. Priebsch, M. Frizsche and D. Rehder, *Inorg. Chem.*, 1993, **32**, 1844.
- 36 M. Minelli, J. H. Enemark, R. T. C. Brownlee, M. J. O'Connor and A. G. Wedd, *Coord. Chem. Rev.*, 1985, **68**, 169.
- 37 E. C. Alyea and J. Topich, *Inorg. Chim. Acta*, 1982, **65**, L95.
- 38 P. Barbaro, C. Bianchini, G. Scappaci, D. Masi and P. Zanello, *Inorg. Chem.*, 1994, **33**, 3180.
- 39 G. E. Meister and A. Butler, *Inorg. Chem.*, 1994, **33**, 3269.
- 40 A. Messerschmidt and R. Wever, *Proc. Natl. Acad. Sci., USA*, 1996, **93**, 392.

Received 12th February 1998; Paper 8/01226A

